Paper Number: 058

Measurement of the dynamic tip twist angle of an active twist model scale rotor blade

Steffen Opitz*, Johannes Riemenschneider, Frauke Hoffmann, Oliver Schneider

German Aerospace Center (DLR), Lilienthalplatz 7, 38108 Braunschweig, Germany

Abstract

Ever since the early days of helicopter flight vibrations and noise have been issues. One major source for helicopter noise and vibration is the main rotor. Individual blade control (IBC) in general tackles noise and vibration of rotary wing aircrafts. The architecture of IBC systems evolved from actuated pitch links to active flaps and active twist. The active twist blades investigated at DLR (German Aerospace Center) are actuated by piezoelectric Macro Fiber Composite Actuators that are integrated into the skin of the rotor blades. Unfortunately some advantages of the active twist concept like: distributed actuation without big local strains or no moving components are also causing some challenges in the control of the actuation. Even though a feedforward control of the actuation voltage can be realized easily it is quite difficult to find a physical value that is suited to close the control loop. As the angle of attack at the blade tip has a big influence on the trajectory of the vortices the tip twist angle of the blade is identified to be controlled. But since the twist is generated over the whole span of the blade, it is not possible to measure the actuation amplitude at a discrete hinge as for an active flap. The fact that the active twist blades investigated at DLR are model scale blades causes additional challenges due to the high centrifugal forces and the limitations in size. Within this paper the requirements on a measurement system for the detection of the tip twist angle of an active twist blade in model scale will be elucidated. As the next step in the development of the active twist blades at DLR are wind tunnel tests, the system should work at least under wind tunnel forward flight conditions. First two optical measurement methods for the detection of the tip twist at one azimuth position will be introduced and compared. Those techniques are serving as a reference later on. From the intention to control the tip twist in a closed loop, arises the need for a continuous measurement of the tip twist angle. In a first approach accelerometers were used to detect the flap wise accelerations at the leading and trailing edge of the blade tip. The results of those measurements will be compared to the optical reference and the limitations of this principle will be shown. Another way to estimate the motion of the blade tip is the use of strain gauge data. Theoretically the moments measured by the strain gauges can be integrated to a deformation when the distribution of the stiffness is known. The database that is needed for these investigations was established during an extensive measurement campaign performed in the DLR rotor test facility in Braunschweig between January 2009 and April 2009. The challenges related to the analysis of this data for an active twist rotor blade will be pointed out. A possible solution will be investigated and restrictions on the applicability of this measurement method will be made.

Key Words: active twist, rotor dynamics, twist measurement

Introduction

Its the capability of hovering that makes the helicopter a unique aircraft. Unfortunately the principle of the rotating wings has some major disadvantages. The main rotor of a helicopter is one of the major sources for helicopter noise and vibration. During more than 100 years of ambitious research and development the levels of those disturbances were diminished drastically, but there is still potential for improvements. Besides passive means to tackle discomfort and fatigue active approaches are becoming more and more investigated in order to meet the rising requirements. Further on gains in performance are predicted by the use of such systems. In the past the active rotor control evolved from the higher harmonic control to the individual blade control [1–4]. It was the development of smart materials and new actuators that enabled the possibility to integrate the actuators into the blade [5–8]. The use of mainly piezoelectric instead of hydraulic actuators reduced the overall weight of the system

*(E-mail: Steffen.Opitz@dlr.de)

significantly. The first active blades incorporated stack actuators to drive trailing edge flaps [9–11]. But those systems have some disadvantages. The discrete edges of the flap are generating additional vortices and drag. Further on the mechanical mechanism is subject to wear and is causing additional maintenance effort. The principle of active twist is expected to be able to overcome these drawbacks. The blade is twisted over its whole length without any discrete edges or change in profile. As the actuation mechanism is distributed over the blade span and directly integrated into the structure there are no big local stains or moving parts that have to be maintained. A comparison of active flaps and active twist in given by Derham [12].To make a final assessment of this new technology the active twist has to prove its performance in wind tunnel and whirl tower tests [13, 14]. The german aerospace center (DLR) is investigating model scale blades to validate simulation codes and to answer the questions concerning noise, vibration and performance benefits. Therefore the blade motion is of interest and has to be measured during the tests. Later on it is intended to realize a closed loop control that uses the measured tip twist as feedback signal. For this purposes optical and strain gauge based methods are intended to be used. This paper focuses on the challenges related to measurement of the torsional deformation of an active twist blade.

Design and Instrumentation

The active twist rotor blade that is investigated in this paper is the fourth of a series of Mach scaled BO105 blades with a scaling factor of 1/2.5. Thus it is named AT4. The rotor has a radius of $R = 2m$ and a chord length of $c = 0.121m$. In order to reach the Mach tip number of the BO105 rotor the nominal rotor speed has to be augmented to $f = 17.38Hz$. Like the full scale reference the blade features a C-spar a rectangular planform and a linear pretwist. The active twist is generated by 26 Macro Fiber Composite (MFC) actuators that are embedded into the upper and lower skin of the blade. These Actuators, that are using the d_{33}-effect, are generating a directed strain within 45° to the blade axis. As the strain is generated in the main stress direction of torsion the blade is forced to twist. The actuation mechanism is spread over a large area of the blade skin. This enables the possibility to generate the integral twist deformation without any big local strains. The control laws usually used to improve noise, vibration and performance characteristics have frequency contents between 2/rev and 6/rev. This frequency range comprises the first torsional eigenfrequency of the blade. It could be shown in former investigations that at higher frequencies the maximum tip twist is not reached for an in phase operation of all actuators [15–17]. Hence it might be beneficial to switch off some actuators or to operate them with 180° phase shift. To ensure a maximum of control flexibility each actuator can be operated individually but to reduce the number of high voltage slip rings in the rotor hub the actuators were arranged in segments. During the test campaign the blade was operated using 3 independent amplifiers.

In addition to the actuators the blade is also equipped with strain gauge sensors. 6 full bridges for torsion moments and 6 half bridges for flap bending moments are distributed over the blade span (see figure 1). Like the actuators the strain gauge instrumentation is also integrated directly into the rotor blade skin. This is advantageous for the manufacturing but is also related to some challenges in the post-processing of the strain gauge data as will be shown later on. Further on the tip of the blade incorporates two LED's that are used to measure the tip deflection in flapping and torsion.

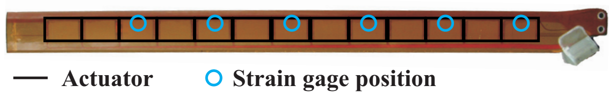

Figure 1: AT4

Blade motion measurement techniques

It is the high rotor speed that makes the measurement of the motion and the deformation of the blade a challenging task. Many measurement methods that can be used in the laboratory (e.g. laser vibrometer, triangulation sensors,...) are not suited to capture the motion of a elastic rotor blade that spins at $1043rpm$. The most common techniques that were already realized in experimental rotor testing are:

- acceleration measurements
- optical measurements
- analysis of strain gauge data

Accelerometers

The centrifugal forces at the tip of the model scale active twist blade are enormous. This becomes obvious when the centrifugal accelerations are calculated.

$$\begin{aligned} a_{centrifugal} &= \Omega^2 \cdot R = (2 \cdot \pi \cdot 17.38Hz)^2 \cdot 2m \\ &= 23850\frac{m}{s^2} = \underline{2431.2g} \end{aligned} \quad (1)$$

As the sensitive axis of accelerometers used to measure flapping or torsion is normal to the rotor disc the huge static centrifugal acceleration is almost orthogonal to the sensor axis. But even a small inclination of the blade tip would cause a considerable output signal. To avoid the saturation of the sensor the measurement range has to be selected adequate. Unfortunately this is counterproductive for the measurement of the blade twist movement where very small accelerations have to be detected. Only to get a feeling for the order of magnitude of the accelerations that are caused by a twist amplitude of $\theta = 1°$ with a frequency of $f = 17.38Hz = 1/rev$, a realistic distance of $d = 35mm$ is assumed.

$$x(t) = d \cdot \tan(\theta) \cdot \sin(\omega \cdot t) \quad (2)$$
$$a(t) = \omega^2 \cdot x(t) \quad (3)$$
$$\widehat{a} = \omega^2 \cdot d \cdot \tan(\theta) \approx \underline{0.74g} \quad (4)$$

In addition to the challenges caused by the centrifugal field there are also strict limitations of installation space. The blade has a chord length of $c = 121mm$ and a maximum thickness of $t = 14.5mm$. As the chordwise distance d between sensor and elastic axis is proportional to the measured accelerations that are generated by the twist of the blade, the sensors should be placed near leading and trailing edge where the airfoil thickness is much smaller. During the testing of a former active twist blade (AT2) it was tried to use two accelerometers integrated at the leading and trailing edge close to the blade tip (see figure 2). The tip twist measured with the ac-

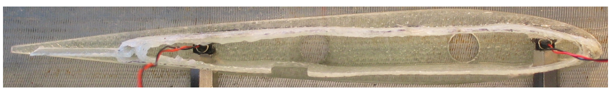

Figure 2: acceleration sensors at blade tip of AT2 blade

celerometers was compared to an optical measurement of the blade tip motion. Looking at figure 3 it can be seen that neglecting the measurement at $f = 5/rev = 87Hz$ the qualitative result for the excitation of different higher harmonics can be recognized but the order of magnitude is not matching

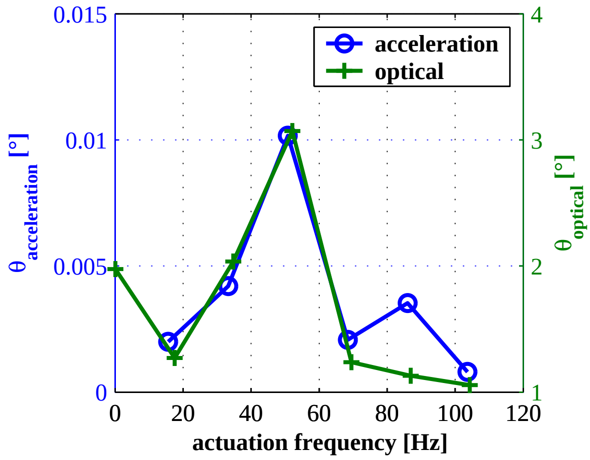

Figure 3: comparison optical and acceleration measurement of blade tip twist

at all. Due to the high centrifugal forces orthogonal to the measurement axis the calibration can not be guaranteed. Furthermore it might be possible that the piezo ceramic material is even partially depolarized where the compressive strain becomes too high. During later tests the sensors did not show any signal at all. Opening the housing of the sensors it was found out that the brittle ceramic was completely crumbled. For this reason it is very difficult to measure the tip motion using accelerometers in this specific case. Consequently further testing focused on optical and strain gauge methods.

Optical methods

In former wind tunnel campaigns optical measurement techniques were used to capture the blade motion. As Stereo Pattern Recognition (SPR) is used as a reference in this paper a brief description of the method is given. The technique is based on the well known principle of photogrammetry. Two cameras are taking pictures from the same scene but from different directions. If the same object is recognized in both pictures its position in space can be calculated. To simplify the detection of the objects, markers can be used. Prior to the measurement the measurement volume is calibrated [18]. A second technique that can be used to measure the blade motion is the Projection Moiré Interferometry (PMI). This method was used during the testing of an active twist blade in the Langley Transonic Dynamics Tunnel in 2000 [19, 20]. Those optical methods are well established but they have several disadvantages:

- not real time capable
- low azimuthal resolution (limited by measurement time)

- complex camera setup to avoid shading

During the testing of the blade another very simple optical measurement system was used. The system is composed by two LEDs that are integrated into the tip of the blade and a azimuth triggered camera. The camera is positioned in the plane of the rotor disc and focusing on the tip of the blade. Each time the blade passes by a picture of the tip is taken with a shutter time of $1/100000^{th}$ of a second. This results in a black picture with two bright dots caused by the LEDs. Those pictures are very easy to post-process and can be used to calculate the motion of the blade tip [14]. Unfortunately the measurement with this system is limited to one sample per camera and revolution. To sum up it can be stated that the optical motion measurement techniques are not suited to deliver a feedback signal for a closed loop control.

Analysis of strain gauge data

Strain gauges are not able to measure the absolute position of the blade. They can only measure deformations. Thus rigid body motions can not be captured. Nevertheless for known boundary conditions (displacement and angle at the hinge) the blade deformation can be integrated from the root up to the tip and the displacement can be predicted. Unfortunately the measurement errors are also integrated and accordingly the maximal uncertainty is located at the tip. Prior to the centrifugal testing the bending stiffness EI_{flap} and the torsional stiffness GI were determined and the strain gauge bridges were calibrated to bending moments $M_{b_{flap}}$ and torsion moments M_t in a bench test. Finally the flap displacement $z(r)$ and torsion $\theta(r)$ displacement can be calculated using:

$$z(r) = -\iint_{r_{hinge}}^{R} \frac{M_{b_{flap}}(r)}{EI_{flap}(r)} dr \qquad (5)$$

$$\theta(r) = \int_{r_{hinge}}^{R} \frac{M_t(r)}{GI(r)} \cdot dr \qquad (6)$$

As $M_{b_{flap}}(r)$ and $M_t(r)$ are only known at the position of the strain gauges, the integral has to be calculated numerically. In general the strain gauges are arranged in wheatstone bridges. The AT4 incorporates half bridges to measure the flap deformation and full bridges to capture torsion. For both types of bridge circuits the arrangement of the single gauges allows to suppress output signals due to the centrifugal forces at least theoretically. But due to small and unavoidable misalignments of the gauges the compensation is not perfect and the mean value of the bridge often changes slightly with the rotor speed. As the influence of the centrifugal force to the bridge mean value is hard to calibrate only the dynamic data is analyzed. This paper is focused on the determination of the dynamic tip twist angle. The calculation of the flap deformation using the strain gauge data is analog to passive blades. This is state of the art and will not be shown.

Challenge

Even though the calculation of blade deformation seems straight forward for passive blades this changes for the investigated active twist blade. The moments that are causing the torsional deformation of an active twist blade can be divided into two groups. The first one comprises the moments that are causing the torsional deformation of regular passive blades too (e.g. aerodynamic moments, inertia moments,...). These moments and the resulting deformation will be referred to as "passive" in this paper. The second group contains the moments that are generated by means of the integrated actuators. Those moments and the corresponding deformations will be referred to as "active". Having a look at the signals of the torsion strain gauges, it is obvious that the signal that is generated by an active twist is much higher than the bridge output that is caused by a passive twist of the same magnitude (see figure 4). Figure 4 shows the linearized

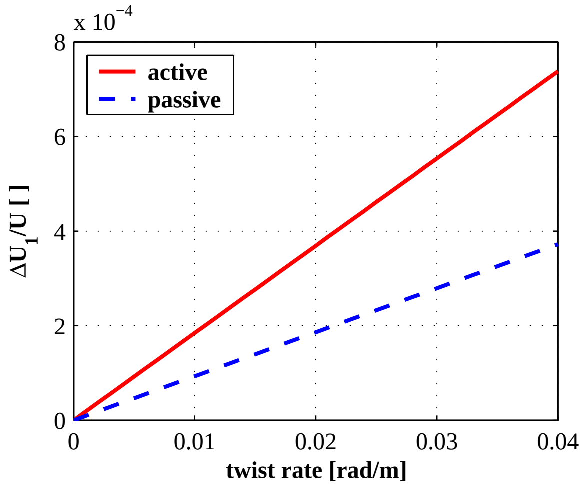

Figure 4: output of torsion bridge 1 as a function of twist rate

dependency of the normalized strain gauge voltage from the twist rate. When the twist is generated by the actuators the strain distribution alters from the one that is generated by an external moment that twists the blade. This can also be visualized using the results of finite element calculations (see figure 5). Analog to the visualization of the pressure

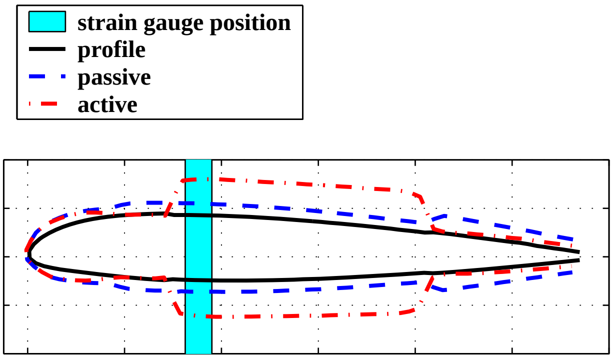

Figure 5: active and passive distribution of +45° strain

distribution in the aerodynamics, figure 5 shows the strain in 45° direction at the inner surface of the skin (location of the gauges) in one cross section of the blade in case of active and passive twist. Both distributions were normalized to the twist rate. In the case of active twist (red line)the location of the actuators is clearly cognizable since the strain level is significantly augmented. Further on it can be seen that the elongation of the piezo ceramic fibers is causing a range with only small or even negative strain right in front and behind the actuators. Thus a strain gauge at this position would be unsuited to detect an active twist deformation. The strain distribution caused by an external passive moment (blue line) is much more uniform. The distribution shows two small kinks at the position were the solid part of the C-spar ends and another two where the actuator ends. The reason for the different sensitivities is the proximity of actuators and sensors. As already mentioned the actuators as well as the strain gauges are integrated into the skin of the rotor blade. The actuators are located at the outer surface of the Glass Fiber Reinforced Polymer (GFRP) skin while the sensors and the wiring were placed on the inner surface of the skin. Remember that the actuators are covering a big amount of the surface area thus the sensors can only be placed underneath or near the MFCs. Hence actuators and sensors were only separated by $0.25mm$ of GFRP.

The consequence is that if the strain gauge data is the only information available and the reason for the deformation is unknown the twist can not be predicted unique. Thus it can be stated that an algorithm is needed to correct the torsion strain gauge values for the case that the strain gauges are located underneath an actuator that is operated. As the flap strain gauges are compensated for torsion deformations due to the bridge circuit they are not affected.

Approach

The basic idea is to calculate the torsion deformation of the blade using equation 6. To calculate the torsional moment M_t that has passive (e.g. aerodynamics, inertia) and active components (MFC actuators), three transfer functions have to be determined:

1. Actuator voltage to strain gauge voltage $H_{\frac{U_{sg}}{U_{act}}}$
2. Strain gauge voltage to passive moment $H_{\frac{M_{pas}}{U_{sg}}}$
3. Actuator voltage to equivalent actuator moment $H_{\frac{M_{act}}{U_{act}}}$

Knowing these transfer functions and assuming a linear system M_t can be calculated using the following procedure. As the actuator voltage U_{act} is known the amount of strain gauge signal that is produced by the actuators $U_{sg_{act}}$ can be calculated using the first transfer function.

$$U_{sg_{act}} = H_{\frac{U_{sg}}{U_{act}}} \cdot U_{act} \tag{7}$$

Please note that the hysteresis of the piezoelectric material is neglected at this point. Next the measured strain gauge signal $U_{sg_{meas}}$ is corrected by subtracting $U_{sg_{act}}$.

$$U_{sg_{corr}} = U_{sg_{meas}} - U_{sg_{act}} \tag{8}$$

The second transfer function is used to determine the passive moment M_{pas} out of the corrected strain gauge voltage.

$$M_{pas} = H_{\frac{M_{pas}}{U_{sg}}} \cdot U_{sg_{corr}} \tag{9}$$

Finally the equivalent actuator moment M_{act} that is calculated from the actuator voltage and the third transfer function is added to the passive moment.

$$M_{act} = H_{\frac{M_{act}}{U_{act}}} \cdot U_{act} \tag{10}$$

$$M_t = M_{pas} + M_{act} \tag{11}$$

Once again the hysteresis is neglected. The procedure proposed above is a frequency domain approach and has one major disadvantage: the transfer functions have to be determined. This is not trivial. It is not possible to excite the blade with a dynamic external moment to gather the dynamic response of the strain gauges without causing inertial moments. The same problem arises when the other transfer functions are to be determined for frequencies exceeding the quasi static range. For this reason two simplifications have to be made. First

of all it was assumed that the amplitude response is constant over the frequency. The second initial assumption is that there is no phase shift between input and output. These simplifications are state of the art for the calibration of strain gauges to external passive moments (transfer function no.2). The application of these simplifications to the other transfer functions is motivated by the dynamic characteristics of piezoelectric actuators. As piezoelectric actuators can be used up to frequencies in the ultrasonic range the investigated frequencies can be regarded as quasi static for the actuator material.
These simplifications are reducing the transfer functions to static gain values. The first two gain values can be obtained by applying a static or quasi-static actuator voltage respectively an external moment and simply measuring the strain gauge output. The third transfer function is determined in two steps. First the twist rate due to an actuator voltage is measured. In a second step the torsional stiffness of the section of interest is determined using an external moment and dividing it by the measured twist rate. Multiplying the active twist rate from the first measurement with the stiffness yields in the equivalent active moment of the actuators as a function of the actuator voltage.

Test setup

The blade testing was performed in an extensive measurement campaign that was performed in the DLR rotor test facility in Braunschweig between January 2009 and April 2009. The blade was tested on a fully articulated rotor hub under zero thrust and $F_z = 250N$ hover conditions. As only one single blade was tested a counter weight was used to balance the rotor (see figure 6). Originally the hub is designed to test a four bladed rotor. Since the weight of two blades is missing the rotor weight was reduced significantly. Due to this mass reduction a resonance of the test rig moved near the nominal speed of the rotor. To avoid this resonance the blade was tested at $950rpm$ which is about 90% of the nominal rotor speed. To reduce the risk of an actuator faillure the MFCs were operated in the range of $U_{act} = -500V \ldots +700V$ which is 60% of their maximum operating range. The data aquisition system took 128 samples per rotation for 32 revolutions. In addition to the data aquisition of the rotor test rig Stereo Pattern Recognition was used to measure the blade motion for a substantial part of the performed tests. The SPR cameras were azimuth triggered and are located underneath the rotor disk. 28 ultraviolet reflecting markers were painted at the lower side of the blade. They were illuminated by 20 arrays of pulsed ultraviolet LEDs (see figure 6). It is advantageous to use ultraviolet light since disturbing light effects and unintended reflections are avoided. Each SPR camera is averaging 48 pictures that were taken of the same oscillation state. The accuracy of the marker position recognition depends on the resolution and angular set-up of the cameras and on the marker shape and size. For the present conditions the theoretical resolution reaches 0.1 mm in x-, y- and z-direction. In case of a marker distance of $d_{marker} = 84mm$ the resulting torsion angle accuracy is $\theta_{res} \approx 0.14°$. The camera focused on the LEDs at the blade tip is located at the same azimuth position as the SPR cameras. As for zero thrust the rotor conditions are axially symmetrical the different oscillation states of the blade can be captured by changing the phase of the actuation. One period of the actuation was assembled using 8 phase settings. This eases the experimental effort since the position of the cameras does not need to be changed. As soon as thrust is added a strong 2/rev component can be observed in the strain gauge data. Hence the influence of the test rig and its support to the rotor aerodynamics is disturbing the axial symmetrie and the simplified measurement procedure is no longer practicable.

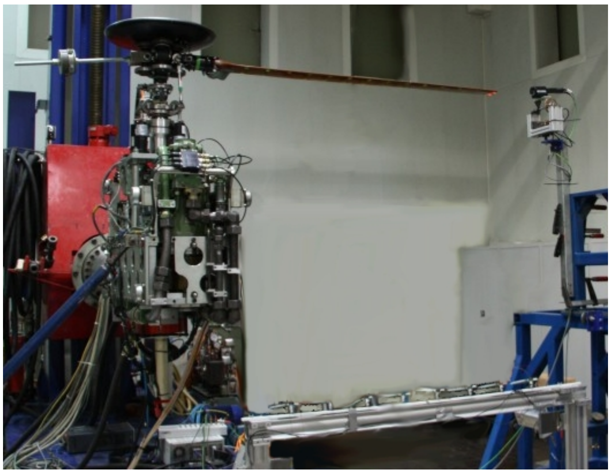

Figure 6: AT4 on rotor test rig

Results

The SPR-measurement and the optical measurement of the tip twist were used as reference to assess the performance of the proposed correction algorithm. The measurement of the blade tip deflection via the LEDs was used to validate the SPR data. Looking at the figures 7 to 10 it is obvious that both optical measurement methods correlate

very well.
The test cases that have been chosen for evaluation are covering a wide range of test scenarios. They comprise actuation frequencies from $1/rev \ldots 7/rev$ operating all actuators with the same voltage signal, segmented actuation where the outer segments are switched off successively and inversely phased actuation of different segments. As already mentioned the azimuthal resolution of the optical methods is quite below the sampling rate of the strain gauge data. As the observed oscillation state was set using the phase of the actuation signal the whole actuation period is obtained from 8 successive measurements. Due to the higher sampling rate there is strain gauge data available in between the optical measurements. The amount of "oversampling" of the strain gauge data depends on the actuation frequency. Like the optical measurements the strain gauge data is also assembled from 8 successive measurements using the strain gauge information located in the vicinity of the azimuth where the cameras are triggered.
To motivate a later modification of the proposed algorithm it is helpful to compare the deformation predicted with and without correction to the optical reference. The following figures show the twist deformation over rotor azimuth ψ and rotor radius r. The results using the algorithm proposed so far will be labeled: "simple correction". The deformation calculated from the strain gauge data will be labeled: "sg".
The frequency corresponding to the first torsion mode of the blade is located at approximately 3/rev. For excitation frequencies below this frequency the uncorrected twist deformation seems to be overestimated but the phase shift to the reference is rather small. In this frequency range the simple correction algorithm reduces the mean deviation between strain gauge prediction and SPR reference to $\Delta\theta_{mean} \approx 0.3°$ (see figure 11). This image changes when the excitation frequency exceeds the first torsional eigenfrequency. A remarkable phase shift between uncorrected twist estimation and reference becomes apparent (see figure 8). This error in phase is diminished through the correction but unfortunately the algorithm produces overestimated twist amplitudes. If the frequency is augmented to 6 or 7/rev the twist results computed from the strain gauge measurement with or without correction are not looking reasonable anymore (see figure 9). The mean deviation between the corrected strain gauge measurement and the optical reference becomes bigger than $\Delta\theta_{mean} > 0.4°$ (see figure 11). Regarding the small amplitudes that are achieved by this highly dynamic actuation this deviation is not acceptable. For an actuation below the first torsional eigenfrequency of the blade the approach delivers acceptable results. But the simple correction algorithm proposed so far is not able to correct the prediction of the deformation in a satisfactory manner as soon as the excitation frequency exceeds the first eigenfrequency in torsion. At this point is has to be kept in mind that the transfer functions were approximated by simple static gain values and no phase

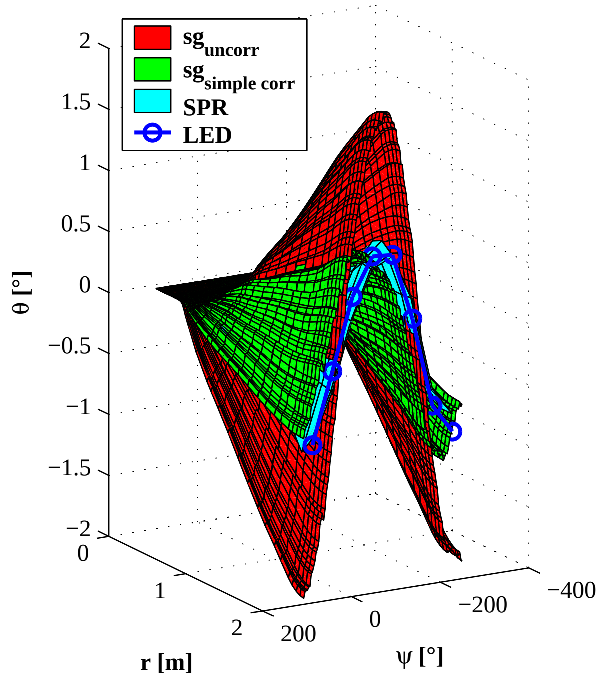

Figure 7: 1/rev twist deformation, all actuators active

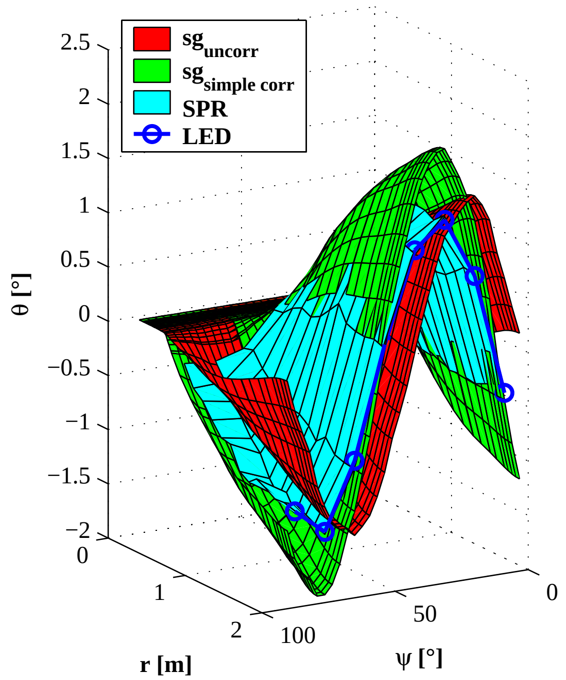

Figure 8: 4/rev twist deformation, all actuators active

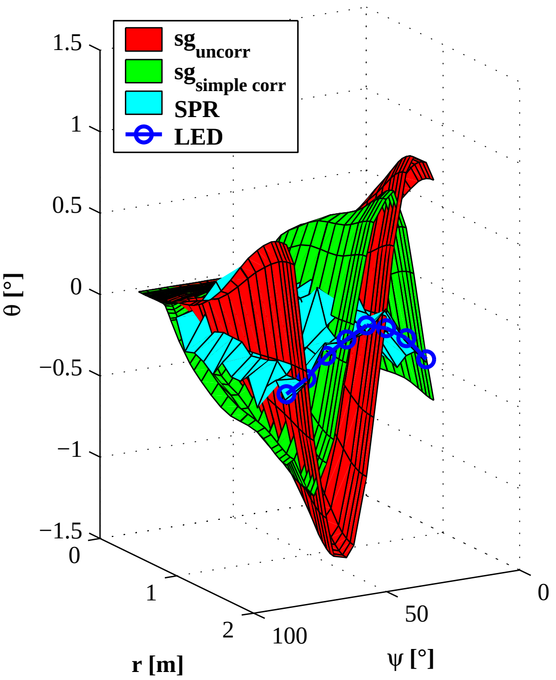

Figure 9: 6/rev twist deformation, all actuators active

shift is regarded. This is an accepted approach for the measurement of the moments in passive blades as well. The blades are calibrated statically and the external moment is assumed to be in phase with the measured strain gauge voltage. Hence the approximation of transfer function no.2 defined above is valid.

The phase shift between the deformations measured with the strain gauges and the optical references changes with frequency. This is the case for the uncorrected data as well as for the data corrected with the algorithm proposed so far. The logical consequence is to add a frequency dependent phase shift to the correction in order to match the reference. The amplitude response is still expected to be constant over frequency. The phase shift φ_{shift} was applied to the actuation voltage U_{act} that is used to calculate the amount of strain gauge signal that is produced by the actuators and the actuator moment.

$$U_{act_{mod}} = \widehat{U}_{act} \cdot \cos\left(n \cdot \Omega \cdot t + \varphi_{shift}\right) \qquad (12)$$

The value for the phase shift was determined in an optimization minimizing the deviation between SPR measurement and strain gauge prediction. The mentioned test cases are divided into two groups. The optimal phase setting was determined for the frequencies from 1/rev to 7/rev and all actuators active. The test cases with segmented actuation were used to validate the phase setting that was found. In a first approach the output voltages of all three amplifiers were provided with individual correction phase values. Of course the optimization was able to fit the data of the test cases with very small errors but no trend over frequency or amplifier could be identified. The phase values seemed to scatter around different constant values over frequency for the three amplifiers. This shows that it is possible to fit the data from the strain gauge measurement to the SPR data in order to get estimates for the deformation in between the coarse measurement points of the optical measurement but the intention of the strain gauge measurement is to have a second method that is calibrated once and afterwards capable to predict the dynamic twist without the presence of the SPR data. Thus a rule has to be found how to set the correction phase as a function of frequency and amplifier. Since no significant trend over the amplifiers was identified the next step was to apply the same correction phase to the voltage of all three amplifiers. This time the phase values seemed to scatter around a linear trend over frequency but the trend had a very small slope. The parameters of the trend line were determined and the test cases with different actuation segments activated were analyzed. As the sensitivity of the correction phase to the frequency was quite small it was investigated whether the phase shift used for the correction can also be set to a constant value over frequency. The comparison to the calculations with the linear trend showed that there is no significant improvement by the usage of the linear dependency. Especially the test cases that were not used for the optimization showed smaller deviations when the simple constant phase value was used. An example for the efficiency of the final correction algorithm using a constant phase value for all amplifiers, frequencies and segment combinations can be found in figure 10. A more general overview of the performance of the algorithm is given by figure 11. The beneficial effect of the empirically applied phase shift for higher frequencies is evident. Finally the test cases that were not used to determine the value for the correction phase can be used to assess the algorithm. Figure 12 shows the mean deviation of the test cases with segmented $3/rev$ actuation. As the maximum tip twist decreases with a reduction of the actuated segments the absolute deviation without correction becomes smaller for those cases. For all test cases the mean deviation did not exceed $0.2°$ which is almost in the range of the accuracy of the SPR reference. Further more the maximum deviation showed to be smaller than $0.5°$. Looking at the results it is obvious that the amplitude is matched better than this. The biggest deviations occur due to slight phase shifts in the region where the sine wave has the steepest slope. Probably this

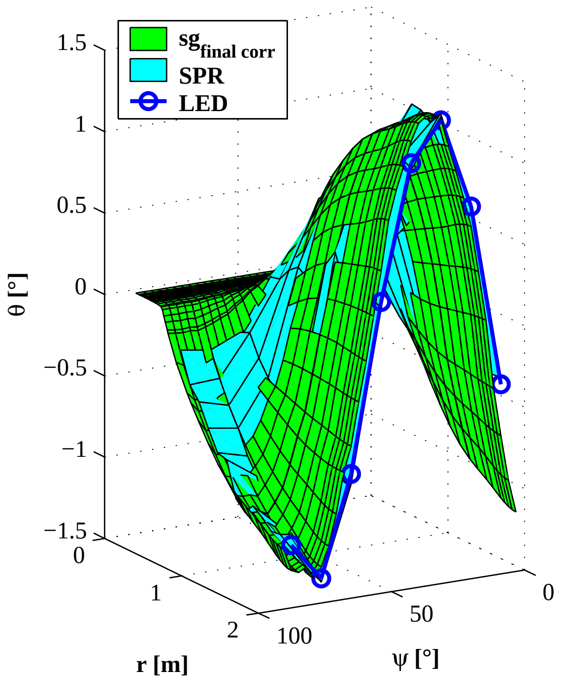

Figure 10: 4/rev deformation with final correction, all actuators active

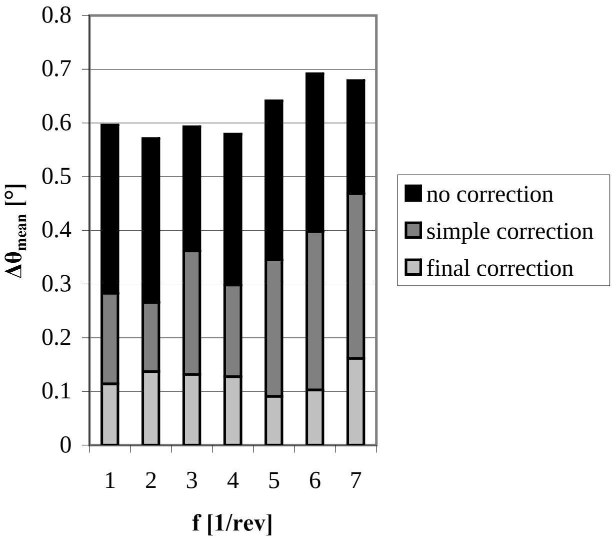

Figure 11: mean twist deviation as a function of actuation frequency, all actuators active

effect can be further diminished when the nonlinear behavior of the piezo ceramic material is regarded since the piezoelectric hysteresis is distorting the sinusoidal shape of the strain signal. Consequently the actuator voltage that is used for the correction should be modified in shape too. But this will be the content of future investigations.

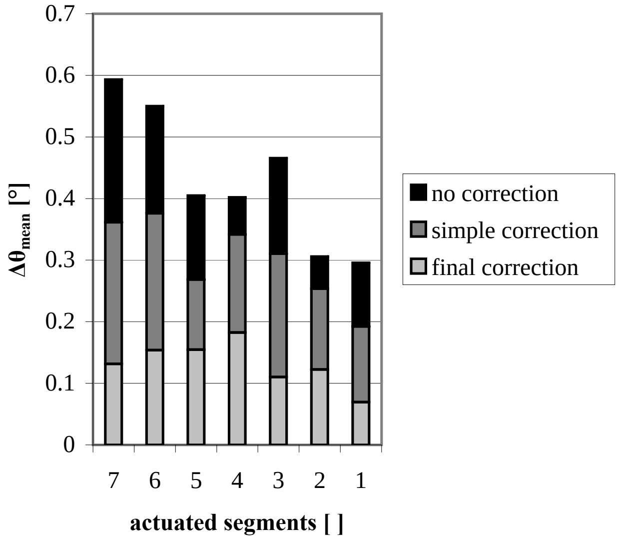

Figure 12: mean twist deviation as a function of activated segments, 3/rev actuation

Conclusion

Within this paper the challenges arising with the prediction of twist deformation of an active twist blade were elucidated. The reason for those difficulties were explained and the analysis of strain gauge data was investigated in detail. Therefore a simple correction algorithm was proposed. To improve the quality of the correction the algorithm was extended by an empirical phase shift. The results were compared with two independent optical measurement methods. Finally it can be stated that the suggested method is capable to correct the disturbing influence of the actuators and the strain gauge data can be used to predict the tip twist. The next steps will be the consideration of the piezoelectric hysteresis and the verification that the algorithm can be used in real time.

Acknowledgment

The authors would like to thank all colleagues for their engagement that was needed to make the measurement campaign a success. Special thanks goes to the DNW for performing SPR measurements and post-processing the data.

References

[1] W. R. Splettstoesser, K. J. Schultz, R. Kube, T. F. Brooks, E. R. Booth, G. Niesl, and

O. Streby. Bvi impulsive noise reduction by higher harmonic pitch control: Results of a scaled model rotor experiment in the dnw. 1991.

[2] R. Kube. Aeroelastic effects of helicopter vibration reduction by higher harmonic control. International Forum on Aeroelasticity and Structural Dynamics, 1991.

[3] U. T. P. Arnold and G. Strecker. Certification, ground and flight testing of an experimental ibc system for the ch-53g helicopter. American Helicopter Society, Montreal,Canada,2002.

[4] Christoph K. Maucher, Boris A. Grohmann, and Peter Jänker. Review of adaptive helicopter rotor blade actuation concepts. Adaptronic Congress, Göttingen, Germany, 2006.

[5] R. Barrett and F. Brozoski. Adaptive flight control surfaces, wings, rotors and active aerodynamics. 1996.

[6] P. C. Chen and Inderjit Chopra. A feasibility study to build a smart rotor: induced-strain actuation of airfoil twisting using piezoceramic crystals. In *Smart Structures and intelligent Systems*, volume 1917, 1993.

[7] H.P.Monner, S.Opitz, J.Riemenschneider, and P.Wierach. Evolution of active twist rotor designs at dlr. In *16th AIAA/ASME/AHS Adaptive Structures Conference*, Schaumburg, USA, 2008.

[8] J. Riemenschneider, S. Opitz, P. Wierach, H. Mercier des Rochettes, L. Buchaniek, and D. Joly. Structural design and testing of active twist blades - a comparison. In *35th European Rotorcraft Forum*. 35th European Rotorcraft Forum, Hamburg, Germany, 2009.

[9] Francois Toulmay, Valentin Klöppel, Francois Lorin, Bernhard Enenkl, and Jacques Gaffiero. Active blade flaps - the needs and current capabilities. 57th Annual Forum of the American Helicopter Society, Washington, D.C., USA, 2001.

[10] Friedrich K. Straub and Dennis K. Kennedy. Design, development fabrication and testing of an active flap rotor system. 61st Annual Forum of the American Helicopter Society, Grapevine, USA, 2005.

[11] Dieter Roth, Bernhard Enenkl, and Oliver Dieterich. Active rotor control by flaps for vibration reduction - full scale demonstrator and first flight test results -. 32nd European Rotorcraft Forum, Maastricht, Niederlande, 2006.

[12] R. Derham, D. B. Weems, M. B. Mathew, and R. C. Bussom. The design evolution of an active materials rotor. American Helicopter Society, 2001.

[13] J. Riemenschneider, S. Keye, P. Wierach, and H. Mercier des Rochettes. Overview of the common dlr/onera project 'active twist blade'. Marseille, Rotorcraft Forum, Sep Marseille, France, 2004. Marseille, Rotorcraft Forum, 30th European Rotorcraft Forum.

[14] J. Riemenschneider, P. Wierach, S. Opitz, and F. Hoffmann. Testing and simulation of an active twist rotor blade. In *Adaptronic Congress*. Adaptronic Congress, Göttingen, Germany, 2007.

[15] Peter Wierach, Johannes Riemenschneider, Steffen Opitz, and Frauke Hoffmann. Experimental investigation of an active twist model rotor blade under centrifugal loads. In *33rd EUROPEAN ROTORCRAFT FORUM*, Kazan, Russia, 2007.

[16] F. Hoffmann, S. Opitz, and J. Riemenschneider. Validation of active twist modeling based on whirl tower tests. American Helicopter Society International, Grapevine, USA, 2009.

[17] Steffen Opitz, Johannes Riemenschneider, and Hans P. Monner. Modal investigation of an active twist helicopter rotor blade. In *ICAST - International Conference on adaptive Structures and Technologies*, Hong Kong, China, 2009.

[18] O Schneider, van d. B. G. Wall, and K. Pengel. Hart 2 blade motion measured by stereo pattern recognition (spr). In *American Helicopter Society 59th Annual Forum*, Phoenix, Arizona, 2003.

[19] M. L. Wilbur, P. H. Mirick, W. T. Yeager, C. L. Langston, C. E. S. Cesnik, and S. Shin. Vibratory loads reduction testing of the nasa/army/mit active twist rotor. American Helicopter Society, Washington DC, USA, 2001.

[20] M. L. Wilbur, W. T. Yeager, and M. K. Sekula. Further examination of the vibratory loads reduction results from the nasa/army/mit active twist rotor test. In *American Helicopter Society 58th Annual Forum*. American Helicopter Society International, Inc, Montréal, Canada, 2002.